Chapter 8

Construction and Analysis of HR Diagrams

In this Chapter we combine our optical photometric and spectroscopic datasets to assemble HR diagrams for several Ae/Be regions. We begin with a general description of our procedure for constructing HR digrams and then present our results for several regions. Our goal is to translate relative luminosities and temperatures into relative ages and masses, via comparison with pre-main sequence evolutionary tracks. As we will show, however, the absolute stellar age and mass calibrations are quite uncertain due to differences in the predictions of various sets of theoretical models. We include in our discussion, a comparison between two different pre-main sequence evolutionary prescriptions, using newly computed luminosities and temperatures for members of the Orion Nebula Cluster over the mass range $0.1 - 40$ $M_{\odot}$. From this comparion, we assess the accuracy to which we can determine cluster age and mass distributions. Having quantified the uncertainties in individual stellar masses, we then present in Chapter 9 a statistical method for investigating the consistency of observed stellar mass spectra with those predicted by universal mass functions.

8.1 Placement of Young Stars in the log T_{eff} - log $(L/\ L_{\odot})$ Plane

To place the stars in an HR diagram, effective temperatures are assigned from our spectral types using the temperature scale determined by Cohen & Kuhi (1979). The uncertainties in log T_{eff} are $\lesssim 0.03$ for F-M stars, but slightly larger for early-type stars where the temperature scale is a steep function of spectral type. In order to compute luminosities, we employ the method of applying

bolometric corrections to reddening-corrected I_C-band magnitudes. The determination of *stellar* luminosities from data in the red optical region offers the following advantages: 1) the extinction correction at I-band is approximately 60% of its value at V-band; 2) the bolometric correction at I-band is small for late-type stars (expected to dominate our cluster samples), which are seen close to their peak flux; and 3) the contribution from circumstellar emission processes at I-band appears to be minimized in comparison to other wavelength regimes. We belabor this last point in the following discussion.

The most critical step in the luminosity calculation is correction for line - of - sight extinction. We proceed in this exercise with caution, as we have shown that many of the stars found nearby Ae/Be stars show the observational signatures of being surrounded by remnant circumstellar disks / envelopes. The excess continuum emission at infrared *and optical* wavelengths in well-studied young star / disk / envelope systems is understood as follows. Infrared excesses over photospheric flux values are produced both by dust reprocessing of optical and ultraviolet stellar photons, and by viscous accretion (in approximately 50% of the cases) of material moving inward through a disk. Optical excesses are produced by energy released in a boundary layer as the accreting material lands on the central star. Correcting for interstellar extinction towards a young star possibly surrounded by a disk thus involves determining the reddening at wavelengths where nonphotospheric flux contributions are minimized. Amongst the set of well-studied young stars with accretion disks, objects of all masses less than about 5 $M_\odot$ seem to have disk and boundary layer contributions minimized around 9000 $\AA$; these sources are best dereddened by computing (R_C-I_C) color excesses.

We determine the extinction towards the stars for which we have spectral types using

$$A_{I_C} = 0.61 \times A_V = 2.90 \times [(R_C - I_C) - (R_C - I_C)_o],$$

where the constant is calculated by interpolating the extinction law of Rieke & Lebovsky (1982) onto the Cousins photometric system. Intrinsic stellar colors are taken from Johnson (1966) and translated into the Cousins system using the relations of Bessell (1979). If the effects of accretion are strong enough to affect even the R,I bandpasses, our de-reddening scheme will be inaccurate and cause underestimated extinction values leading to underestimated luminosities. We also acknowledge that the presence of anomalous and/or variable extinction could jeopardize our ability to properly de-redden stars. Finally, we compute luminosities using the distances given in Table 1.1 and the bolometric corrections of Hartigan, Strom, & Strom (1994), Code *et al.* (1976), and Mihalas & Binney (1981) which are transformed to the Cousins I_C-band, as appropriate.

Uncertainties in log $(L_*/L_\odot)$ are typically ≤ 0.15, when spectral classification errors are translated into errors in calculated extinctions and assumed bolometric corrections; we note that an error of 0.5 mag in A_V translates into an error of 0.12 in log $(L_*/L_\odot)$. Other effects which may alter the intrinsic position of a star in the HR diagram include those of rapid stellar rotation, unresolved multiples, and mass loss – each of which causes a star to seem brighter and somewhat redder than it actually is. Although quantitative error assessments are difficult, the importance to assigned masses and ages of these effects increases with mass and with proximity to the main sequence. Typical color-magnitude variability trends of young stars (see, *e. g.* Herbst *et al.* 1994) suggest additional uncertainties in the luminosity determination from a single photometric measurement at an unknown brightness state, of ± 0.12 in log $(L_*/L_\odot)$. A final, systematic, source of error is that due to the uncertain distances to the Ae/Be stars, and thus to the clusters under consideration here.

8.2 Results for Selected Regions

We show in Figures 8.1 and 8.2 our HR diagrams over the inner 0.167 pc for the BD +40° 4124 and the Lκ Hα 215 regions. We show in Figure 8.3 our HR diagram over the inner 0.55 pc of NGC 7129. The information contained in these HR diagrams is discussed below for individual regions. We have chosen these regions for presentation as they are the ones in our sample for which our spectroscopic survey is most complete (see Table 5.1).

The pre-main sequence evolutionary tracks and age isochrones of D'Antona and Mazzitelli (1994, model 1) are shown over the mass range from 0.1 $M_\odot$ to 2.5 $M_\odot$. The 4 $M_\odot$ and 5 $M_\odot$ mass tracks are those of Swenson *et al.* (1994, model F) and the 10 $M_\odot$ and 20 $M_\odot$ mass tracks are those of Ezer & Cameron (1967). Although recent revisions to the pre-main sequence tracks have been necessary, these changes have been primarily due to improvements in the convection prescription and in the molecular opacities; understanding of radiative track physics has not changed since the calculations from these older papers were done (although see discussion below on issues related to the stellar "birthline"). Thus the use of a heterogeneous set of tracks for masses over which pre-main sequence evolution is largely radiative, as we have done here, should not be problematic. We note, however, that one of the artifacts of combining different sets of tracks is the small jump in the isochrones near the convective/radiative transition. The observational zero-age main sequence interpolated from Morton & Adams (1968) and Balona & Feast (1975) is also shown in these Figures and corresponds quite well to the theoretically computed end of the pre-main sequence phase down to 0.7 $M_\odot$. Below 0.7 $M_\odot$ there is some disagreement between observational and various theoretical zero-age main sequences, suggesting that further refinements in pre-main sequence evolutionary codes may still be required (see section 8.3 for further discussion). We now discuss the results for each of the

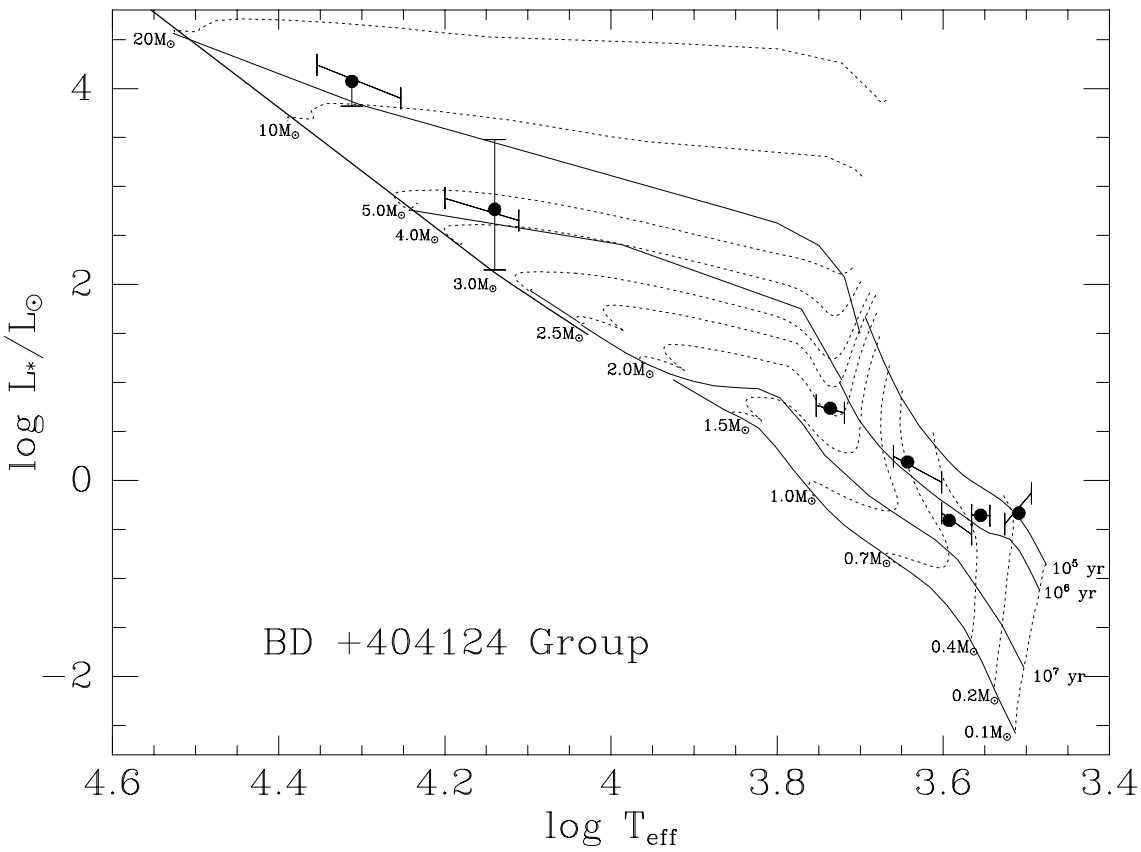

Figure 8.1. *HR diagram for the BD +40° 4124 region.* Superposed are the zero-age main sequence and the pre-main sequence evolutionary tracks of 1) D'Antona & Mazitelli (1994, model 1); over the mass range from 0.1 $M_\odot$ to 2.5 $M_\odot$; 2) Swenson *et al.* (1994, model F) from 4 $M_\odot$ to 5 $M_\odot$; and 3) Ezer & Cameron (1967) from 10 $M_\odot$ to 20 $M_\odot$. Error bars are calculated assuming a random error of ± 1 spectral subclass in addition to any uncertainty in the assigned type. The mean age of the optically visible stellar aggregate surrounding BD +40° 4124 is less then 1 Myr with an age spread from 0.1-3 Myr. The ratio of the number of stars with mass greater than 1 $M_\odot$ to the number of stars with mass less than 1 $M_\odot$ seems unusually over-represented in higher mass stars. Hα emission is seen from 100% of the stars represented on this Figure.

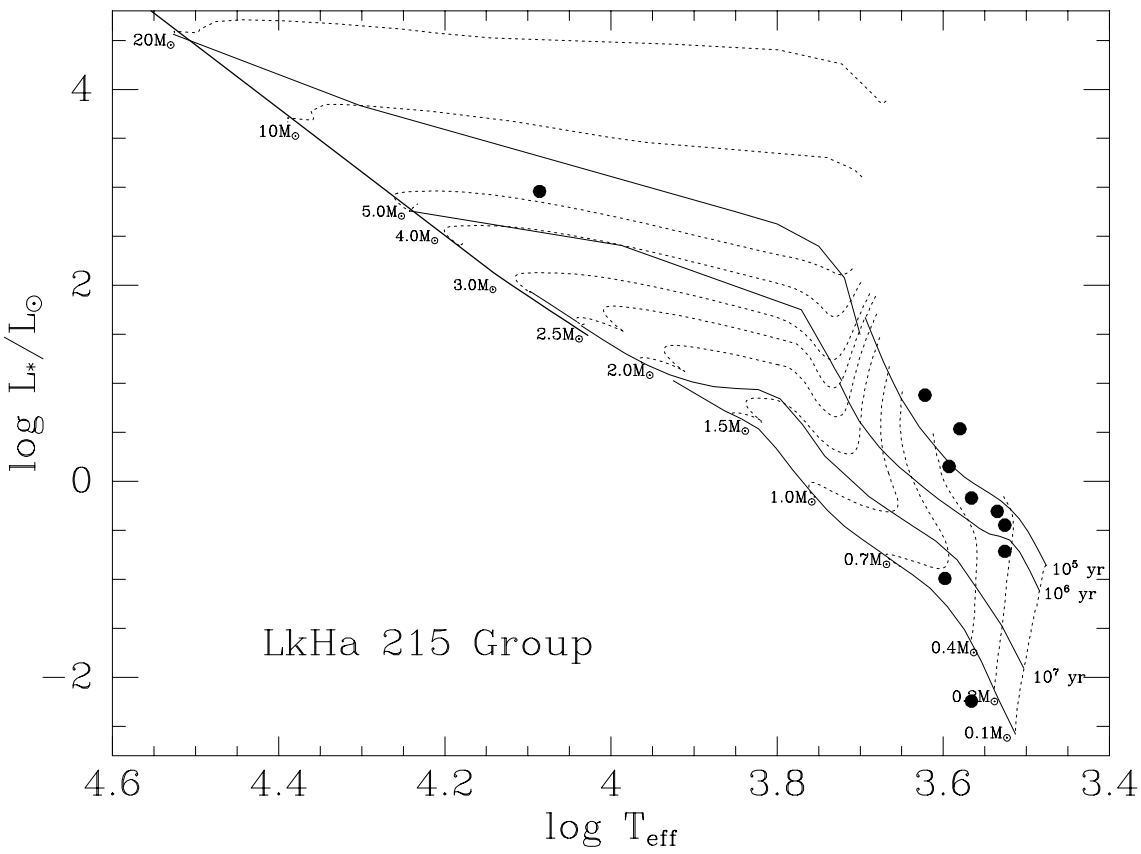

Figure 8.2. *HR diagram for the* LK Hα *215 region.* Superposed lines are the same as in Figure 8.1. The mean age of the optically visible stellar aggregate surrounding LK Hα 215 is less then 0.1 Myr with an age spread from $< 0.1 - 2$ Myr. Other than the Ae/Be star, no other intermediate-mass stars populate this aggregate. Hα emission is seen from 90% of the stars represented on this Figure.

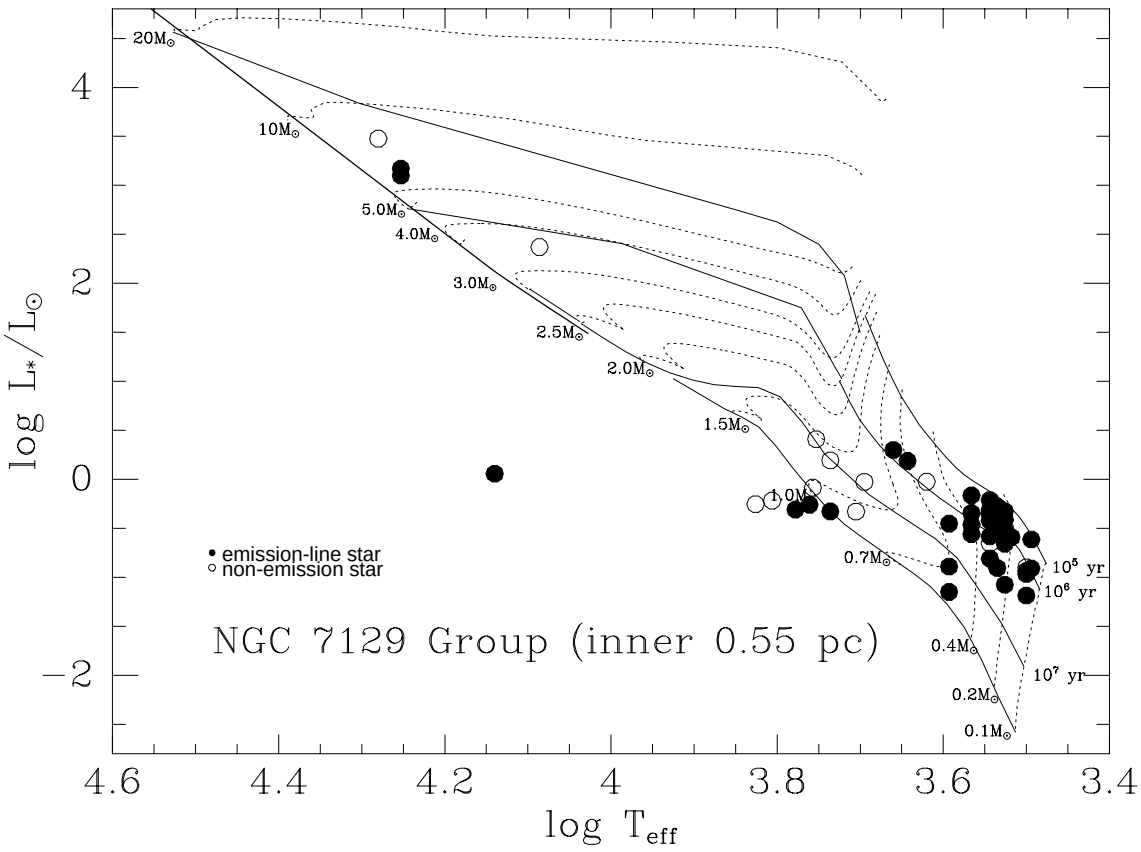

Figure 8.3. *HR diagram for the* NGC *7129 region.* Superposed lines are the same as in Figure 8.1. The mean age of the optically visible stellar aggregate is about 1 Myr with an age spread of perhaps 3 Myr for low-mass stars; for slightly higher-mass stars the mean age is apparently much older (see text). Stars with Hα in emission are indicated with filled symbols.

three regions separately, basing our analysis on a literal interpretation of the pre-main sequence tracks as presented.

8.2.1 The BD +40° 4124 Group

From Figure 8.1 we see that the optically visible members of the BD +40° 4124 aggregate span a range of masses, from about 13 $M_\odot$ to 0.2 $M_\odot$. There are 5 member stars with masses $M > 1M_\odot$ (2 of which are high-luminosity continuum-plus-emission stars and are not shown on this diagram) but only 4 member stars with masses $M < 1M_\odot$. Thus there appears to be an unusually large fraction ($> 50\%$) of intermediate- and high-mass stars in this isolated star-forming core. We explore the robustness and significance of this finding in Chapter 9.

The mean Kelvin-Helmholtz age of the optically visible stellar aggregate is about 1 Myr, with a range from about 0.1-3 Myr. While there is a modest age spread, it is clear from our completeness limits in the I_C-(R_C-I_C) diagram that there are no stars older than 3 Myr. Finally, we find no evidence for an ordered sequence of star formation as a function of stellar mass (*e. g.* from low to high or from high to low); high- and low-mass stars are forming relatively simultaneously.

8.2.2 The Lk Hα 215 Group

From Figure 8.2 we see that, like in the BD +40° 4124 region, the optically visible members of the Lk Hα 215 aggregate span a range of masses, from about 6 $M_\odot$ to 0.2 $M_\odot$. However, unlike in the BD +40° 4124 region, our spectroscopic survey near Lk Hα 215 identified no additional group members with masses $M > 1M_\odot$. The ratio of high- to low-mass stars seems consistent with that in the solar neighborhood.

The mean Kelvin-Helmholtz age of the optically visible stellar aggregate is about 0.1 Myr, with a range from about $< 0.1 - 2$ Myr. We note that there are

two low-luminosity stars which seem significantly older than the remainder of the cluster stars, but we reject the accuracy of these ages on the grounds that both of these stars have Hα in emission and one of the two has a significant near-infrared excess; we think it likely that the presence of veiling emission causes severe underestimation of the extinction towards these sources and thus underestimated luminosities.

8.2.3 The Lk Hα 234 Group (NGC 7129)

From Figure 8.3 we see that at least 5 stars in the central part of NGC 7129 have masses $M \geq 3$ M$_\odot$ and that the range of stellar masses extends to near the hydrogen-burning limit.

As in the BD +40° 4124 and Lk Hα 215 regions, the HR diagram for NGC 7129 shows a spread in age for the late-type stars of about 3 Myr. The mean age for the low-mass population is about 1 Myr. Slightly higher-mass stars seem characteristically older (3-10 Myr) than the lowest-mass stars. Early-type stars have ages consistent with those of the late-type stars. We do not yet understand the origin of this trend in apparent stellar age with stellar mass, but explore it further in the next section.

8.2.4 Other Ae/Be Groups and Next Steps

In addition to those groups mentioned above, there are 10 other Ae/Be clusters in which at least some classification spectra have been obtained. We give a summary of the approximate spectral types of members of these clusters in Table 5.1, but do not present HR diagrams for these regions. Spectroscopic data continue to be collected, and upon the completion of this process we will be able to discuss the characteristic age and mass distributions in these other aggregates as we have done for the BD +40° 4124, Lk Hα 215, and NGC 7129 groups.

However, having derived photospheric temperatures and luminosities to the best of our observational ability in at least a few regions, we would now like to reliably combine pre-main sequence evolutionary theory with our data in order to investigate the *detailed* distributions of stellar masses and ages in the Ae/Be clusters. We have already stated basic results on masses and ages for the three Ae/Be groups which have been fully analyzed to date, based on a strict interpretation of the evolutionary tracks. However, concern regarding literal interpretation of the tracks / isochrones arises from several sources, discussed in the next section.

8.3 Understanding Pre-Main Sequence Evolution

Among the uncertainties in our current picture of pre-main sequence evolution are: 1) the as-of-yet unquantified effects of ongoing accretion during the optically visible stage of stellar contraction; 2) uncertainties in the physics under which pre-main sequence stellar evolution proceeds (particularly in the case of low-mass stars); and 3) uncertainties in the initial luminosities and radii with which pre-main sequence stellar evolution begins (particularly in the case of high-mass stars). We address these concerns in turn in the following three sub-sections.

8.3.1 The Unaccounted-for Effects of Ongoing Accretion

First, based on evidence assembled over the past several decades with a wide variety of astronomical techniques, (at least 50% of) low-mass pre-main sequence stars younger than 10 Myr are suspected to be still undergoing accretion processes. The combination of accretion rates derived from optical veiling studies, accretion mass resevoirs derived from infrared and submillimeter studies, and accretion duration timescales derived from statistical studies of dust continuum excesses in young clusters, implies that during the optically visible pre-main sequence phase,

at least 10% of the final stellar mass is added. However, the detailed effects on stellar evolution in the HR diagram of ongoing mass accretion remain unstudied. In part, this is due to uncertainty regarding how material actually reaches the stellar surface (*e. g.* through spherical accretion, disk accretion, or magnetospheric accretion) and by what process newly added material comes into equilibrium with the rest of the star. We note that the liberation of accretion energy (*e. g.* in a boundary layer or in heating of the disk) is not of concern here as we are interested only in the internal stellar luminosity for purposes of the HR diagram. What is the effect of ongoing accretion for pre-main sequence evolution? The bulk effect must be that accreting stars move across conventional mass tracks and, more importantly, have their chronometers reset as they do so. Specifically, for a fully convective (n = 1.5 polytrope) star which is radiating due to gravitational contraction only,

$$L = \frac{dE}{dt} = \frac{d}{dt}\ \frac{3}{7}\ \frac{GM^2}{R} = \frac{3}{7}\ \frac{GM}{R}\ (2\dot{M} - M\frac{\dot{R}}{R}).$$

If $\dot{M} = 0$ then we can solve for L, which goes as $\tau_{KH}^{-2/3}$ (where τ_{KH} is the Kelvin-Helmholtz or canonical contraction age). If $\dot{M} > M/2\tau_{KH}$ then the luminosity evolution is more rapid. Calculations of equatorial disk accretion by Stringfellow (1989) show that for a star of initial mass 0.2 $M_\odot$ accreting at a rate of 10^{-6} $M_\odot$ yr^{-1}, the increase in internal stellar luminosity is more than an order of magnitude and the corresponding increase in radius is about a factor of two, over the values predicted for a non-accreting star. The luminosity and radius effects are certainly more severe for higher-mass stars and for higher disk accretion rates. These realizations place into question the accuracy to which stellar masses and ages can be interpolated from pre-main sequence tracks and isochrones which do not include these effects. What is needed are computations of pre-main sequence "accretion tracks".

8.3.2 Comparison of Two Pre-Main Sequence Evolutionary Codes

A second concern regarding the literal interpretation of HR diagrams, is that significantly different ages (several Myr or more) and masses (factors of two) can be read from different sets of pre-main sequence evolutionary tracks for stars of a given log $(L_*/L_\odot)$ and log T_{eff} . We illustrate this in Figure 8.4 with an HR diagram of the inner part ($r < 2$ pc) of the Orion Nebula Cluster (ONC; see Appendix C for a discussion of the data). Superposed are the electronically circulated forms of the pre-main sequence evolutionary predictions of 1) D'Antona & Mazitelli (1994) and 2) Swenson, *et al.* (1994) . It is clear that these two sets of evolutionary tracks yield quite different stellar ages and masses for the same set of luminosities and temperatures. Are there systematic differences? In Figure 8.5 we show plots of the stellar ages and masses derived by interpolating between the isochrones and tracks of the previous Figure. Indeed, there are systematic differences as the Swenson, *et al.* (1994) calculations characteristically produce older ages and higher masses (for $M \lesssim 1$ $M_\odot$) in comparison to the D'Antona & Mazitelli (1994) calculations. The offset in age reflects a difference in the "zero point" of the calculations, that is, where in the HR diagram an object becomes self-luminous following the end of the initial accretion stage. The offset in mass is due to differences in the assumed convection and opacities, the effects of which are largest at cool temperatures (note that the two sets of calculations seem to agree for stars on radiative tracks).

8.3.3 A Stellar "Birthline" in the HR Diagram?

A third concern regarding current pre-main sequence evolutionary theory is an apparent trend in Figure 8.4 of stellar age with mass. In Figure 8.6 we plot explicitly the age against the mass for individual stars, for both the D'Antona & Mazitelli (1994) and the Swenson, *et al.* (1994) calculations. We find that, although

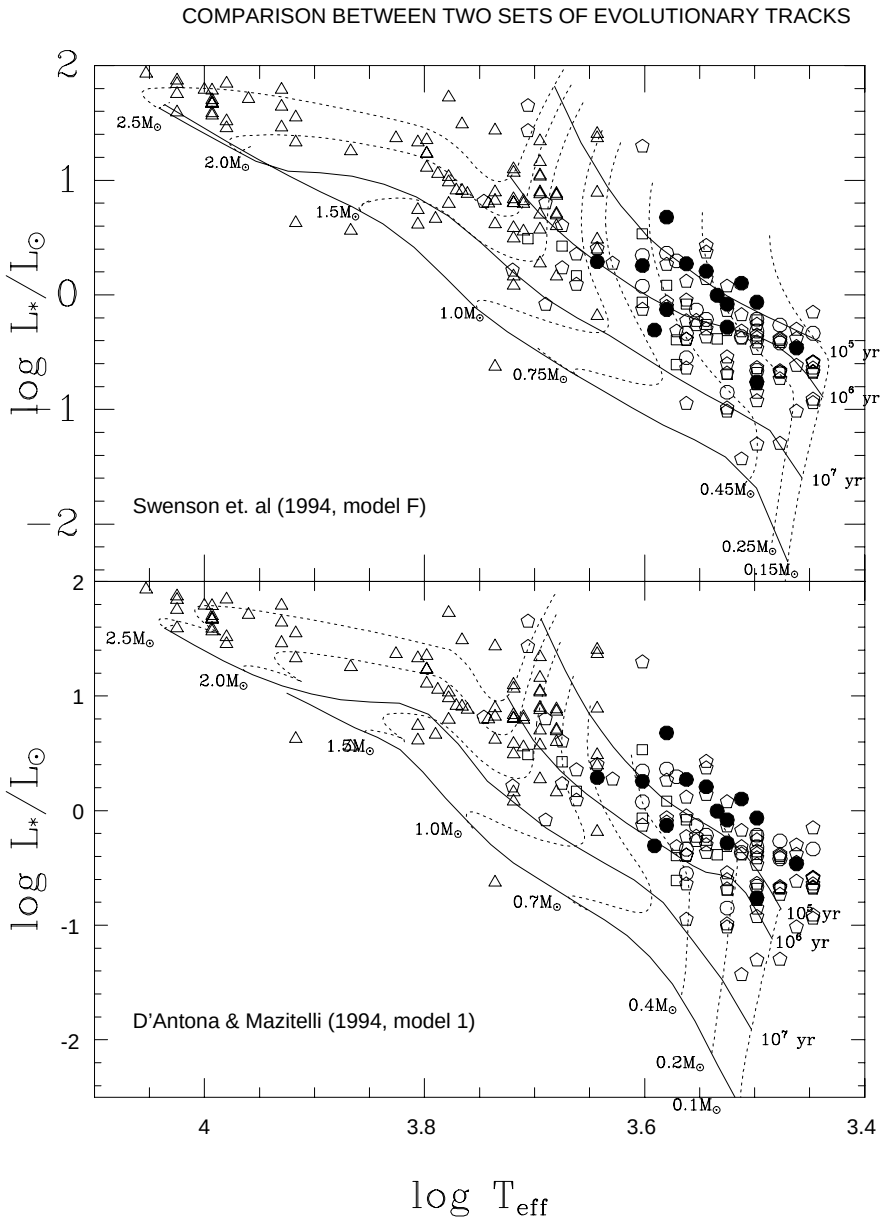

Figure 8.4. *HR diagram for the inner 2 pc of the Orion Nebula Cluster,* $2.5 > M/M_{\odot}$. See Figure 8.7 for a definition of the symbols; filled symbols represent stars in the inner 0.167 pc. Superposed are the pre-main sequence evolutionary tracks over the mass range from 0.1 $M_{\odot}$ to 2.5 $M_{\odot}$ of (bottom panel) D'Antona & Mazitelli (1994, model 1) and (top panel) Swenson *et al.* (1994, model F). These two currently circulating pre-main sequence evolutionary prescriptions yield quite different results on stellar masses and ages when compared with the same set of data, particularly at temperatures $\log T_{eff} < 3.6$.

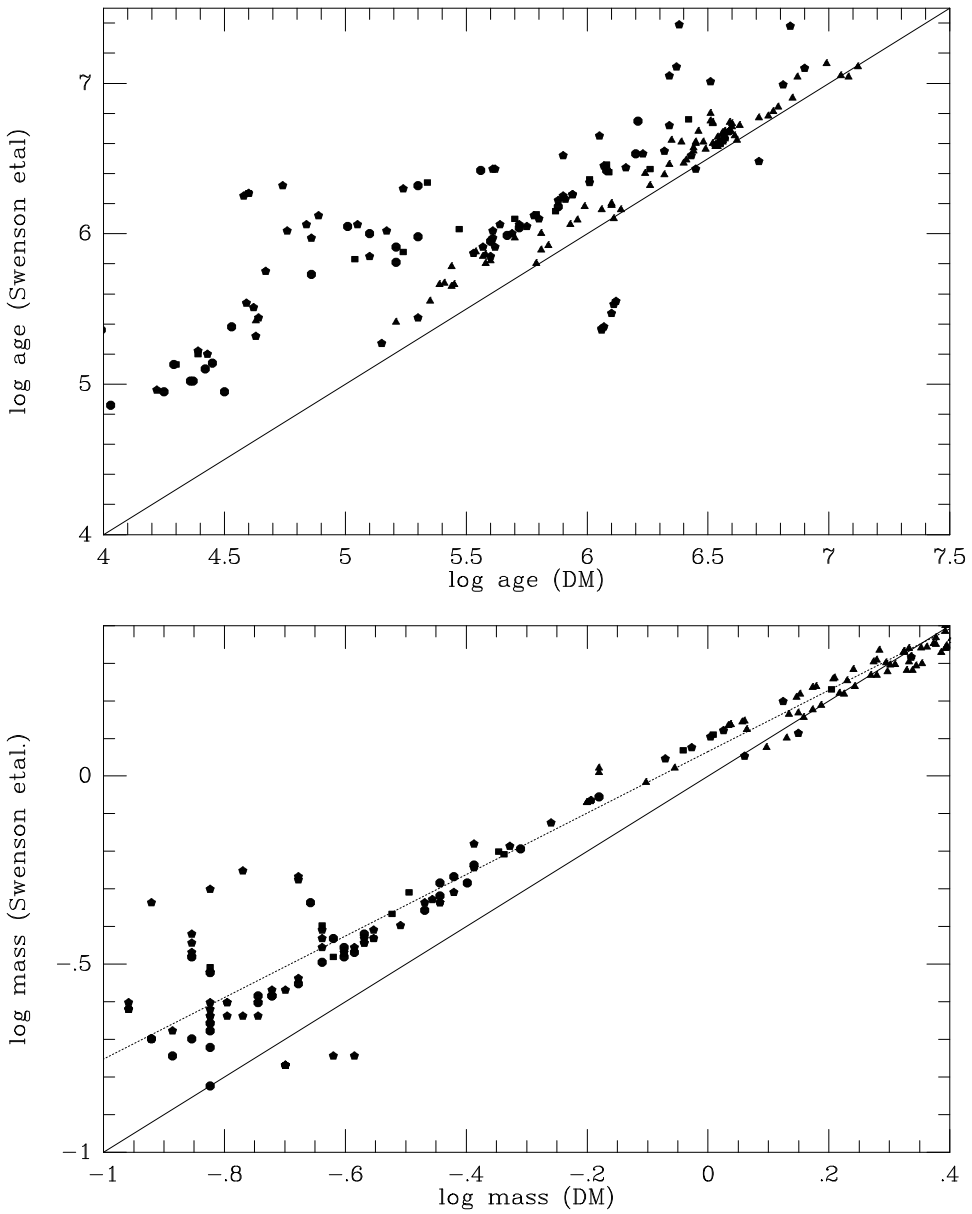

Figure 8.5. *Direct comparison of stellar ages (upper panel) and masses (lower panel) derived from D'Antona & Mazitelli (1994) and Swenson, et al. (1994) evolutionary codes.* See Figure 8.7 for a definition of the symbols. On the lower panel, the solid line indicates a 1:1 relationship while the dotted line is a fit to the data and has slope ≈ 0.8. Above 1 $M_\odot$ the agreement between derived masses and ages for stars of the same luminosity and effective temperature is quite good. Below 1 $M_\odot$ there is significant disparity between these two sets of tracks.

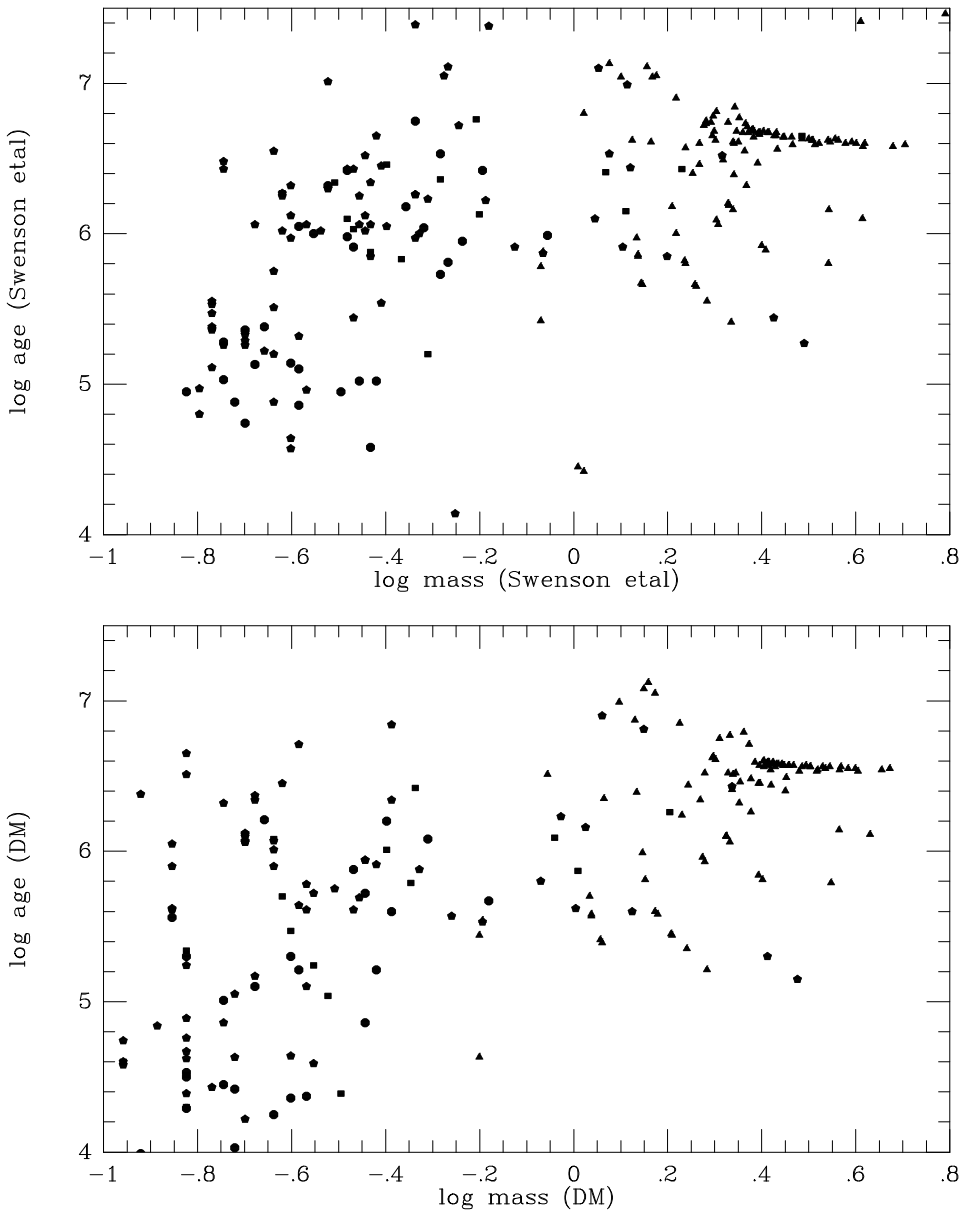

Figure 8.6. *Apparent correlation of stellar age with stellar mass, as derived from existing evolutionary tracks.* See Figure 8.7 for a definition of the symbols. Interpolation of stellar ages and stellar masses from the HR diagrams (Figure 8.4) reveals a nonintuitive trend of increasing age with mass. We suspect this is due to a lack of rigorous understanding of the "zero point" of the tracks, *e.g.* where in the HR diagram an object becomes self-luminous following the end of the initial accretion stage; see text.

the scatter is large, there is some tendancy from the available isochrones for higher mass stars to appear older than lower-mass stars in the same young cluster.

We pursue investigation of this apparent trend of age with mass by plotting (Figure 8.7) the HR diagram for the ONC over its full range of masses, from ≈ 40 $M_\odot$ down to the hydrogen burning limit (see Appendix C for a discussion of the data). The ONC has been venerated in star formation studies as a "classic" case of triggering; however, surprisingly little is actually known about the global properties of its stellar population. Our goal in studying this densely populated region of masssive star formation was to provide context for our investigations of smaller, less well-populated molecular cores containing Ae/Be stars. So as to make comparisons of the stellar age/mass distributions between the ONC and the isolated Ae/Be clusters over the same spatial scale, stars with projected radii $r < 0.167$ pc from $\theta^1 C$ Ori (the most massive of the Trapezium stars) are highlighted in Figure 8.7. Of the 237 stars on this Figure, 19 meet this criterion. Summarizing the appearance of the HR diagram, 1) the low-mass stars populate a region extending in luminosity from near the Hayashi limit to the 2 or 3 Myr isochrone – independent of the cluster radial scale considered; 2) the intermediate-mass stars appear to be characteristically *older* than the lowest-mass stars – we call attention to the lack of stars with masses larger than 2 $M_\odot$ and Kelvin-Helmholtz ages less than 1 Myr; 3) the high-mass stars are on or near the zero-age main sequence, with inferred (although uncertain) ages comparable to those derived for the lowest-mass stars.

Can such an HR diagram be consistent with the presumed triggering scenario for the Orion Nebula Cluster? To answer this question we must examine how we define the "age" of a star. Traditionally, we speak of the Kelvin-Helmholtz contraction age,

$$\tau_{KH} \approx \frac{GM^2}{RL} = \frac{3 \times 10^7}{yr} \frac{(M/\ \mathrm{M}_\odot)^2}{(\mathrm{R}/\ \mathrm{R}_\odot)(\mathrm{L}/\ \mathrm{L}_\odot)}$$

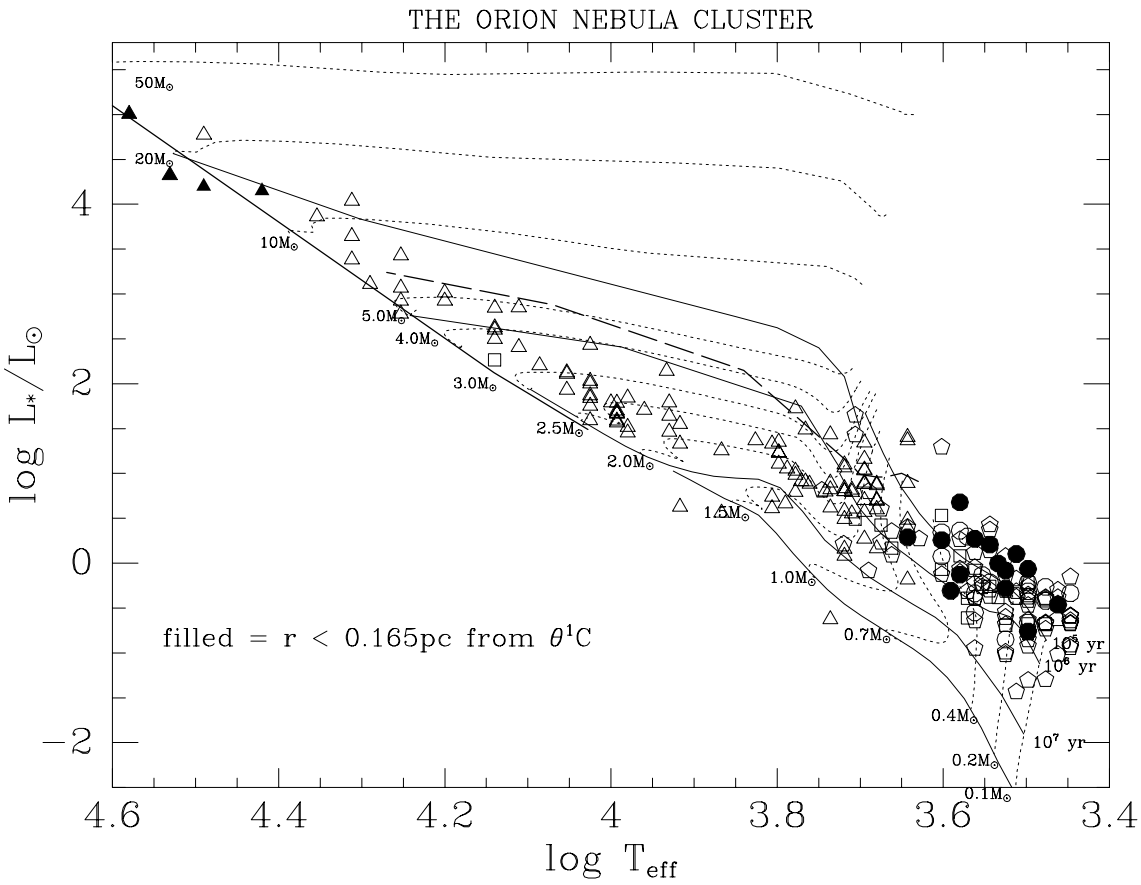

Figure 8.7. *HR diagram for the Orion Nebula Cluster,* $40 > M/M_\odot > 0.1$. Superposed are the zero-age main sequence and the pre-main sequence evolutionary tracks of 1) D'Antona & Mazitelli (1994, model 1) over the mass range from 0.1 $M_\odot$ to 2.5 $M_\odot$; 2) Swenson *et al.* (1994, model F) from 4 $M_\odot$ to 5 $M_\odot$; and 3) Ezer & Cameron (1967) from 10 $M_\odot$ to 20 $M_\odot$. Also shown is the "birthline" computation of Palla & Stahler (1993). All stars are proper motion cluster members. Spectroscopic data was obtained at the KPNO 4m telescope with the HYDRA bench spectrograph while photometric data is from Prosser *et al.* (1994; circles), Herbst *et al.* (1994, private communication; squares), our own CCD study (pentagons), and Walker (1969; triangles); see Appendix C for a discussion of this data set. To enable comparison to the Ae/Be clusters, stars in the inner 0.167 pc are highlighted. Note the lack of stars more massive than 2 $M_\odot$ with Kelvin-Helmholtz ages less than 1 Myr.

which is, simply, the timescale for radiation of gravitational energy during quasi-static collapse. The zero-point of this timescale is set by the temperature (*e. g.* opacity) at which hydrostatic equilibrium is reached for a given mass, derivable from the condition $dP/dr = -g\rho$ and some assumptions about the fully convective nature of the initially collapsing clump. It is assumed that the Kelvin-Helmholtz time is much longer than the sound crossing time, and so thermal conditions are uniform throughout the protostar during collapse. In this approximation, essentially no energy is radiated before the onset of collapse and thus the initial radius is infinite, or at least very large.

However, as first demonstrated by Larson (1969), the collapse of a protostar is non-homologous. Instead of occuring as a quasi-static event, the protostellar clump undergoes free-fall. A dense stellar core rapidly develops and material from the outer regions of the collapse falls onto a growing central protostellar seed which is itself no longer contracting. Since the free-fall time and the sound crossing time are comparable in a cloud near hydrostatic equilibrium the accretion shock propogates outward at the sound speed (Shu, 1977; Stahler, Shu, & Tamm, 1980; Tereby, Shu, & Cassen 1984). For all masses, the initial stellar radii are much reduced from the homologous picture and, furthermore, the contraction times are no longer Kelvin-Helmholtz. Due to the radiation of energy in an accretion shock, the thermal timescales are now different in different regions of the star. Thus effects of the initial accretion episode, whose associated timescale is $\tau_{acc} = M/\dot{M}_{acc}$, must be included. Addition of energy from an accretion shock necessitates that sufficiently massive stars undergo a thermal readjustment which quickly enables them to develop radiatively stable cores. Stars more massive than ≈ 2 $M_\odot$ avoid the convective pre-main sequence stage entirely and are essentially "born" as radiative objects. For stars more massive than 8 $M_\odot$, the Kelvin-Helmholtz timescale is shorter than the spherical accretion timescale; thus

nuclear reactions have begun in the center of the star before dynamical collapse in the outer layers has stopped. All high mass stars are thus predicted to be "born" on the zero-age main sequence, without having passed through a conventional pre-main sequence phase.

Introduction of the term "stellar birthline" in the H-R diagram was made by Stahler (1983) and most recently updated by Palla and Stahler (1993 and references therein). The "birthline" is essentially a prediction of initial stellar radii as a function of mass (*e. g.* a mass-radius relationship) at the instant following the "end" of the initial accretion episode. The R(M) prediction depends on 1) the details, including geometry, of internal deuterium and hydrogren burning; 2) the infall geometry, that is, spherical (Stahler 1983) or disk (Mercer-Smith, Cameron & Epstein 1984) accretion; and 3) the steady-state mass accretion rate during the quasi-static collapse. With a set of pre-main sequence evolutionary tracks, a derived R(M) relationship can be translated into a locus of log $(L_*/L_\odot)$ and log T_{eff} on the HR diagram. In theory this line constitutes a prediction of maximum luminosity as a function of effective temperature, or mass. However, location of "the" birthline is not unique due to the dependence on the infall characteristics. Thus one might imagine the existence of a "birthband" as a function of mass, which accounts for different infall/accretion rates, instead of a "birthline".

What does all of this mean for stellar ages? It is important that the stellar configuration at the end of the main accretion phase translates directly into that with which the star begins its quasi-static contraction towards the main sequence (Stahler, Shu, & Tamm 1980). For low-mass, fully convective stars, this means that the difference between the "appropriate" contraction timescale and the Kelvin-Helmholtz timescale is not much more than a free-fall time (Stahler 1983). For higher mass stars the timescale differences are larger although, as already noted, critically dependent on the assumed infall/accretion rate (*cf.* Figure 2 of

Palla & Stahler, 1993). Based on the above discussion, one might imagine adjusting the evolutionary isochrones to reflect the initial mass-radius relationship. The age of a star then becomes (following Stahler, 1983)

$$\tau = \tau_{isochrone} - \tau_{isochrone,\ initial} + \tau_{acc},$$

where the first term denotes the quasi-static contraction age, the second term denotes the "initial" age at the end of the major accretion phase, and the last term denotes the length of the dynamical contraction phase ($M/\dot{M}_{acc}$). However, if in a cluster either the initial assembly times or the dust clearing times vary systematically with mass, artificial apparent age spreads can result. Additional uncertainty in stellar ages may be introduced by either steady-state or transient elevated (*e. g.* FU Ori-like) accretion during the traditional pre-main sequence contraction stage, as discussed above.

Returning to our results in the ONC, at least qualitatively, the combination of possible pre-main sequence theoretical evolutionary scenarios described above seems consistent with our HR diagram. We find a systematic trend of Kelvin-Helmholtz ages with stellar mass, suggesting that the ages need to be revised downward as a function of mass to account for thermodynamic effects generated in the initial accretion episode. Furthermore, we find a distribution in luminosity corresponding to a spread in age of at least 3 Myr at all masses below 3 $M_{\odot}$ (above this mass stars are close to the zero-age main sequence and we lose age resolution). This suggests one of the following scenarios, either 1) star formation really has been occuring for several million years near the Trapezium, not a particularly appealing alternative given the popularity of the triggering schematic for this region; 2) our ability to place stars in the theoretical log $(L_*/L_{\odot})$ - log T_{eff} plane suffers from large, random luminosity errors corresponding to apparently large age spreads; 3) the luminosity evolution of young, accreting pre-main sequence stars is significantly different from that

advocated by standard theory. Regarding this last point, if stars do indeed move along accretion tracks until joining standard Hayashi or Henyey tracks upon final assembly of the full stellar mass, then without knowing whether a star is finished accreting we do not know which direction it is moving in an HR diagram!

8.3.4 Suggested Tests of Evolutionary Tracks

The evidence provided above on 1) the discrepancies between various modern theoretical pre-main sequence evolutionary prescriptions; 2) the systematic trend of Kelvin-Helmholtz age with stellar mass reflecting lack of certainty regarding "zero age" for a pre-main sequence star; and 3) the lack of knowledge about the luminosity evolution of still-accreting stars, suggests that rigorous observational tests of the theoretical predictions are critical. This is particularly true as observers are inclined to use the theory to translate relative luminosities and temperatures into absolute stellar ages and stellar masses.

One of the first questions we might ask is whether the theoretical calculations accurately reproduce the observed zero-age main sequence. This issue is being addressed by L. Allen, who is attempting to quantify how well theoretical isochrones trace the observed loci of stars in the Praesepe ($\tau = 700$ Myr), Pleiades ($\tau = 70$ Myr), and α Per ($\tau = 20 - 50$ Myr) clusters. These regions are old enough so that intrinsic age spreads should be undetectable, and thus cluster sequences should lie strictly along single isochrones. Preliminary results indicate that in fact isochrones from the available low-mass evolutionary sequences are "crossed" at the low-mass end in these clusters. However, from Prosser *et al.* (1994) we learn that the Swenson, *et al.* (1994) tracks at least match both the Bessell (1991) standard dwarf sequence and the Stauffer & Hartmann (1986) Pleiades main sequence for values of $\log T_{eff} > 3.6$.

Another means of testing pre-main sequence evolutionary codes is with binary stars. Do visual, eclipsing, or double-line binary systems lie along common isochrones, as might be expected if their formation took place as a system (*e. g.* in a disk or pseudo-disk) instead of as individual collapse events in a common cloud core? The issue of coevality was addressed for by Hartigan, Strom, & Strom (1993) for a sample of wide binary pairs in Taurus and Orion. By placing the individual members of visual pairs in the HR diagram using techniques similar to those employed here, coevality to within the errors was established in approximately 2/3 of the cases, but of the remaining 1/3 all systems displayed the trend that the more massive star appeared *older* from the tracks, consistent with the systematic trend we have suggested here from the ONC data. The issue of coevality is being addressed by R. Mathieu, B. Casey, & R. Lee for several eclipsing and double-line binary systems. Eclipsing and double-line pairs can be placed in the HR diagram using only effective temperatures derived from stellar spectra and masses derived directly from orbital elements. This technique for testing the tracks is clearly the most direct and suggests the same trend as found above, although good data are available for just a few systems (Casey *et al.* 1993, Lee *et al.* 1992).

8.4 Conclusions from HR Diagram Discussion

In principle, if the pre-main sequence evolutionary calculations are trustworthy, the construction of an HR diagram for the optically visible members of a young stellar group allows us to constrain the age of the cluster. This information is necessary in the context of our scheme for de-reddening sources without spectra (described in Chapter 7). Summarizing our observational results, from the construction of HR diagrams for optically visible group members, we have found apparent age spreads of several Myr in every region discussed in this

section: BD +40° 4124, Lk Hα 215, NGC 7129, and the ONC, results which we state with reservation due to the theoretical uncertainties.

The purpose of our lengthy discussion above on issues related to the accuracy of available pre-main sequence evolutionary tracks and isochrones, was simply to introduce appropriate caution into interpretations of stellar masses and ages derived from such tracks. Pre-main sequence masses appear to be uncertain, at the 50% level. Pre-main sequence ages appear to be highly uncertain, at a level greater than 100% (several Myr) in the cases of extremely young clusters. This is most likely due to the unknown affects of accretion both during the initial infall phase and during the optically visible pre-main sequence contraction phase. Location of pre-main sequence binary systems with good orbital elements in the HR diagram, under the assumption of constant age, should help discern between various sets of tracks. With this cautionary information in hand, our next task is to investigate the distributions of stellar masses in the Ae/Be clusters.